A conserved photosynthetic cytochrome enhances growth of *Chlamydomonas reinhardtii* in fluctuating light

Darius Kosmützky[1,†,*], Laura T Wey[2], Lauri Nikkanen[2], Aron Ferenczi[3], Joshua M Lawrence[1,4], Alberto Scarampi[1,‡], Attila Molnar[3], Yagut Allahverdiyeva[2], Christopher J Howe[1,*]

1: Department of Biochemistry, University of Cambridge, Cambridge CB2 1QW, UK

2: Molecular Plant Biology, Department of Life Technologies, University of Turku, Turku 20014, Finland

3: Institute of Molecular Plant Sciences, University of Edinburgh, Edinburgh EH9 3BF, UK

4: Yusuf Hamied Department of Chemistry, University of Cambridge, Cambridge CB2 1EW, UK

†: Present address: Sainsbury Laboratory, University of Cambridge, Cambridge CB2 1LR, UK

‡: Present address: School of Life Sciences, University of Warwick, Coventry CV4 7AL, UK

*: Corresponding authors

Abstract

Having at least one of the small soluble electron carriers cytochrome c_6 (c_6) and plastocyanin is indispensable for photosynthesis. It was believed that c_6 had been lost from plants until a ubiquitous and highly conserved homologue, now named cytochrome c_{6A} (c_{6A}), was found in *Arabidopsis thaliana*. In spite of an early suggestion that c_{6A} functioned like c_6 in the photosynthetic electron transport chain it was soon shown to be unable to do so despite the strong structural homology between the two proteins. The function of c_{6A}, and why it is apparently universal in plants and green algae, therefore remained unknown. Here, we show that, in the green alga *Chlamydomonas reinhardtii*, c_{6A} confers a growth advantage under fluctuating light and is crucial for maintaining the light harvesting balance between photosystems I and II in photomixotrophic conditions. We show that in the absence of c_{6A}, the light harvesting balance shifts towards PSII, leading to a more reduced plastoquinone pool and increased photooxidative stress. This study provides insights into how photosynthetic organisms acclimatize to stressful light conditions, indicating that c_{6A} is important for this adaptation. These findings provide a basis for further mechanistic studies on a hypothesized role for c_{6A} in thiol-based redox regulation in the thylakoid lumen, with implications for photoprotection mechanisms such as state transitions.

Main Text

Introduction

The photosynthetic electron transport chain (PETC) is essential for nearly all life on Earth (Fig. 1a). At least one of the soluble electron carriers plastocyanin and cytochrome c_6 is indispensable for the PETC to function (1, 2). A close homologue of c_6, cytochrome c_{6A}, was first discovered in *Arabidopsis thaliana* and later in other plants and eukaryotic algae (3, 4). Whereas plants lost the gene for c_6 and contain only c_{6A}, some eukaryotic algae such as *Chlamydomonas reinhardtii* (*Chlamydomonas*) contain genes for both (5), although c_{6A} is expressed at a low level compared to c_6 or plastocyanin (6, 7). Since its discovery, c_{6A} has been hypothesized to have various functions, including replacement of plastocyanin (3), acting as a safety valve for excess electrons of photosynthesis (7), regulation of generation of reactive oxygen species (ROS) in PSI (8), and being

46 involved in high light signalling (9) or thiol-based redox regulation (10, 11). However, the function
47 of cytochrome c_{6A} remains elusive (7).
48 While c_6 and c_{6A} are homologues, there are structural differences between the two (Fig. 1b). c_{6A}
49 contains a 'loop insertion peptide' (LIP), an insertion with a conserved disulfide bridge in a surface-
50 located and well-defined loop. The LIP is absent from c_6 (10). Assessing the stability of various
51 mutant proteins showed that the LIP is structurally important (12, 13). While a catalytic role for the
52 conserved disulfide bridge within the LIP is uncertain, it is predicted to contribute to the protein's
53 structural stability (13, 14). In addition to the LIP, there are differences in the heme environment
54 of the two proteins, and these contribute to c_{6A} (+71 mV (15)) having a 254 mV lower midpoint
55 potential than plastocyanin or c_6 (+325 mV (15)).
56 Phylogenetic analyses revealed that c_{6A} represents a monophyletic group distinct from c_6 and likely
57 originates from cyanobacterial cytochrome c_{6B}, another homologue of c_6 that has a similar midpoint
58 potential to c_{6A} but lacks the LIP (16). The sequence of c_{6A} is highly conserved across the green
59 lineage, as with plastocyanin, suggesting an important role for c_{6A} within photosynthetic
60 eukaryotes (16). However, the large difference in midpoint potentials renders it highly unlikely that
61 c_{6A} acts as a functional replacement for plastocyanin in plants and algae, as c_{6A} would not be
62 expected to accept electrons from the cytochrome b_6f complex (Fig. 1a). Further, plastocyanin was
63 found to be indispensable even when c_{6A} was overexpressed in *A. thaliana* (1). Additionally, the
64 surfaces of c_6 and plastocyanin are both strongly negatively charged, whereas c_{6A} has a strongly
65 positive surface charge (17). Together with the difference in isoelectric points (plastocyanin: 5.1,
66 c_{6A}: 4.1 in *A. thaliana* (18)) this indicates different interactions.
67 Interactions involving c_{6A} further highlight its distinct role (Fig. 1a). It cannot effectively reduce
68 PSI *in vitro*, making direct interaction between c_{6A} and PSI unlikely (17). Additionally, c_{6A} has
69 been shown to reduce plastocyanin *in vitro* (19) and weak interaction (K_d = 2.01 mM) was detected
70 with plastocyanin using NMR titrations (6), consistent with a transient interaction. Yeast Two-
71 Hybrid assays also revealed interactions of c_{6A} with itself (20), the lumen thiol oxidase LTO1 (21),
72 and the redox-regulated immunophilin FKBP13 (3). LTO1 has been reported to be involved in
73 regulating state transitions via the kinase STT7 (22). Interaction with LTO1 and FKBP13 therefore
74 suggests a luminal localization for c_{6A}, consistent with its detection in the soluble fraction of the
75 thylakoid lumen in *A. thaliana* (23). In *Chlamydomonas*, however, only a chloroplastic localization

76 has been confirmed (6). In *A. thaliana*, c_{6A} was also found to be uniquely localized to sensory
77 plastids in the epidermis and vascular parenchyma rather than mesophyll chloroplasts (24).
78 Photosynthetic organisms require flexibility in their photosynthetic apparatus because they grow
79 under a diverse set of environmental conditions. These include varying light conditions from
80 diurnal cycles to more rapid fluctuations caused by the sun, clouds, canopy, and in the case of
81 *Chlamydomonas*, also soil and water movements. For *Chlamydomonas*, exposure to a 12 s on/12 s
82 off cycle with light intensities of 600-700 µmol photons m^{-2} s^{-1} in photoautotrophic conditions
83 resulted in growth rates reaching only about 30% of those achieved under continuous
84 illumination (25). Additionally, a growth penalty was revealed under fluctuating light with
85 frequencies in the range of 10-100 s on/off (26). In mutant assays using *Chlamydomonas*, various
86 fluctuating light regimes have been employed to determine the function of proteins associated with
87 photosynthesis. These include the important proteins Proton Gradient Regulation 5 (PGR5) and
88 Proton Gradient Regulation Like 1 (PGRL1), both implicated in cyclic electron flow, its regulation
89 or ATP synthase regulation (27), as well as flavodiiron proteins (FLVA/B), which facilitate the
90 Mehler-like reaction (28). Additionally, the qE quenching effector LHCSR3 (29, 30) and plastid
91 terminal oxidase PTOX2 (31) have been implicated in the response to fluctuating light, as mutants
92 of all of these proteins showed a growth deficit under fluctuating light conditions.
93 Here, we present the first in-depth analysis of the connection between c_{6A} and photosynthesis. We
94 show that this highly conserved protein is important for growth under a harsh fluctuating light
95 regime we call DISCO Light and helps maintain the redox balance of the plastoquinone (PQ) pool
96 through its effect on the light harvesting balance between photosystems I (PSI) and II (PSII).
97
98
99 **Results**
100
101 Cytochrome c_{6A} confers a growth advantage under a fluctuating light regime
102
103 To investigate the role of c_{6A} in *Chlamydomonas* we used CRISPR/Cpf1 (32) to create a knock-out
104 of the c_{6A} gene (*CYC4*, Cre16.g670950) in the background strain CC-1883 (WT). The knock-out
105 strain ("c_{6A}-KO") was confirmed through PCR and sequencing (Supplementary Methods &
106 Supplementary Fig. 1a-d). We also generated a c_{6A} overexpression c_{6A}-OE) strain by transforming
107 the c_{6A}-KO strain with a construct that drives the expression of FLAG-tagged c_{6A} from a *PSAD*

promoter. Overexpression was confirmed by immunoblot and RNAseq analysis (Supplementary Methods & Supplementary Fig. 1d-e).

To investigate the role of cytochrome c_{6A} in growth, we tested how *Chlamydomonas* strains grow under various light and trophic regimes. Under continuous light (30 µmol photons m^{-2} s^{-1}), both c_{6A}-KO and WT strains reached similar maximum optical densities (OD_{750nm}) of around 2 in photomixotrophic and ~0.6 in photoautotrophic conditions, with no statistically significant differences (Fig. 1c). We defined continuous light (30 µmol photons m^{-2} s^{-1}) and photomixotrophic conditions as standard conditions for this study.

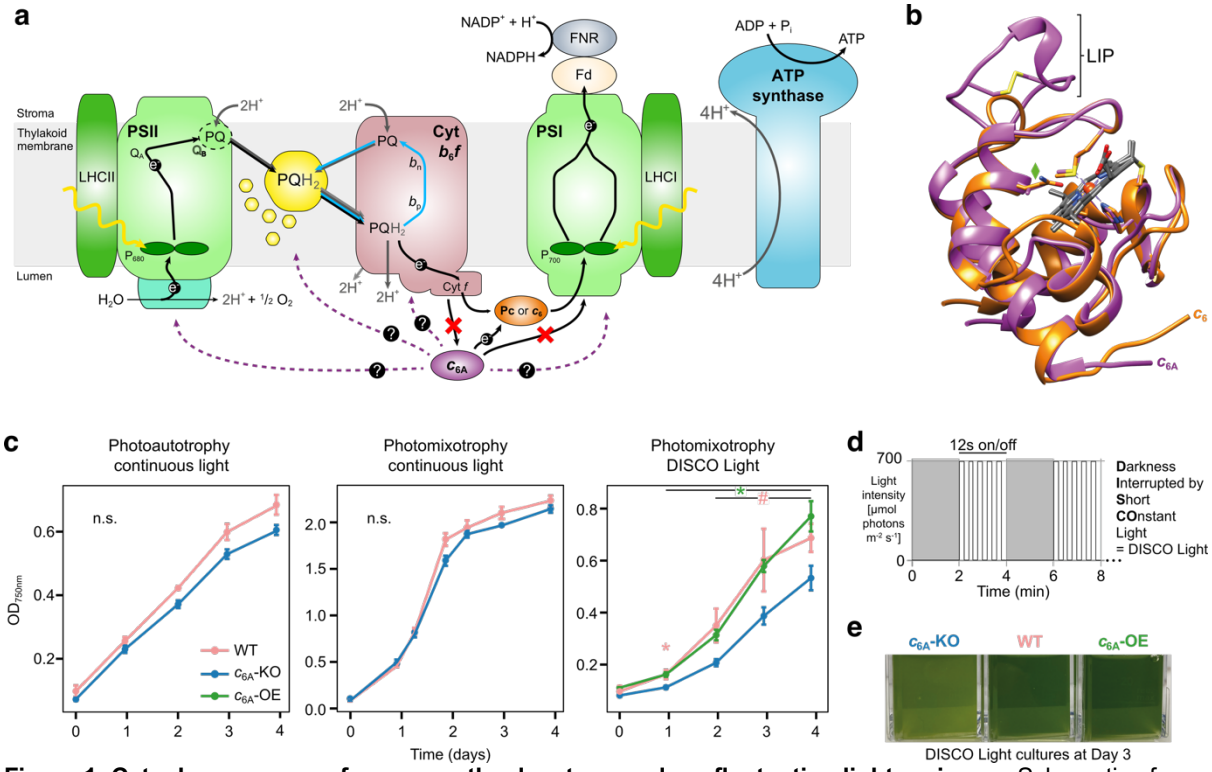

Figure 1: Cytochrome c_{6A} confers a growth advantage under a fluctuating light regime. a, Schematic of the photosynthetic electron transport chain with known (black) and putative interactions (purple) of c_{6A} marked. Proton movement (grey) and the Q-cycle (blue) are shown as arrows. **b**, Overlay of the crystal structures of cytochrome c_6 from *Chlamydomonas* (orange, PDB: 1CYJ (57)) and c_{6A} from *A. thaliana* (purple, PDB: 2CE0 (19)). The position of the LIP is noted with the disulfide bridge formed between the two conserved cysteine residues (yellow sticks). The amino acid residues at position 52 were found to affect the heme environment contributing to the low midpoint potential of c_{6A} compared to c_6 or plastocyanin (stick model and labelled with a green diamond) (15). **c**, Optical density (OD_{750nm}) growth curve of c_{6A} mutant strains and WT under continuous light (30 $\mu mol_{photons}$ m^{-2} s^{-1}) in either photoautotrophy or -mixotrophy and DISCO Light and photomixotrophy (n = 3 biological replicates ±SD). Statistical testing was carried out with repeated measures ANOVA. Post hoc pairwise two-sided t-tests at each time point were performed if the interaction effect of time and strain on OD_{750nm} in the ANOVA was significant ($p_{time:strain} < 0.05$) comparing WT (pink) or c_{6A}-OE (green) against c_{6A}-KO ($p < 0.05$: *, $p \leq 0.1$: #). **d**, DISCO Light (Darkness Interrupted by Short COnstant Light) consists

of alternating 2 min darkness followed by 2 min of high light pulses (12 s high light (700 $\mu mol_{photons}$ m^{-2} s^{-1}) & 12 s darkness). **e**, Visual differences of the c_{6A} mutant and WT cultures of at day 3 of growth in DISCO Light.

We also tested multiple stressful light conditions for their effect on c_{6A}-KO and WT. Only a light regime we named DISCO (Darkness Interrupted by Short COnstant) Light and photomixotrophy led to an observable phenotypic growth difference (Fig. 1c). DISCO Light was devised to expose *Chlamydomonas* to a complex fluctuating light regime covering multiple frequencies, as it consists of two alternating phases: 2 min of darkness followed by 2 min of alternating 12 s high light pulses of 700 $\mu mol_{photons}$ m^{-2} s^{-1} and 12 s darkness (Fig. 1d). c_{6A}-KO grew more slowly and reached lower cell densities than WT under photomixotrophic DISCO conditions (Fig. 1c & e): after one day c_{6A}-KO cultures showed significantly reduced growth (P = 0.029), and by day 3 they were approximately 1.5 times less dense than WT cultures (P = 0.10). The growth penalty in c_{6A}-KO was recovered by overexpressing c_{6A}, with c_{6A}-OE showing significantly higher cell densities than c_{6A}-KO from day 1 (P = 0.024, Fig. 1c & e). In the DISCO light regime without acetate in the medium (photoautotrophy), no strain could grow (Supplementary Fig. 2e).
In photomixotrophy and darkness or continuous high light at the same light intensity as in the DISCO regime (700 $\mu mol_{photons}$ m^{-2} s^{-1}) WT and c_{6A}-KO grew at similar rates (Supplementary Fig. 2a-b). Furthermore, fluctuating light regimes corresponding to elements of the DISCO protocol ("2 min high light & 2 min darkness", and "12 s high light & 12 s darkness"), showed only small differences between WT and c_{6A}-KO that were not part of a consistent trend under either photomixotrophic or photoautotrophic conditions (Supplementary Fig. 2c-d).

Measurements of total chlorophyll concentration and acetate consumption confirmed the phenotypic difference between the strains observed from OD_{750nm} measurements in both standard and DISCO Light conditions (Supplementary Fig. 2f-h). The correlation between total chlorophyll concentration and optical density was similar between WT and c_{6A}-KO. This indicated no difference in chlorophyll concentration per cell between the strains under standard conditions or DISCO Light (Supplementary Fig. 2g). Additionally, measurements of acetate concentration in the

160 growth medium indicated that c_{6A}-KO consumed less acetate, likely because of lower cell densities
161 when exposed to DISCO Light, with differences apparent from day 3 (Supplementary Fig. 2h).
162 These results indicate that c_{6A} is important for growth of *Chlamydomonas* under the high intensity
163 and rapidly fluctuating DISCO Light regime and acetate availability in photomixotrophic
164 conditions.
165
166
167 <u>c_{6A} is likely localized in the thylakoid lumen and does not have strongly bound interaction partners</u>
168
169 c_{6A} was detected in the soluble fraction of the thylakoid lumen in *A. thaliana* (23). In
170 *Chlamydomonas*, however, only chloroplastic localization has been confirmed (6). To determine
171 the subcellular localization of c_{6A} in *Chlamydomonas* further, we performed immunofluorescence
172 microscopy on the c_{6A}-FLAG overexpressing strain (c_{6A}-OE) and its background strain (c_{6A}-KO)
173 grown under standard conditions. In the negative control (c_{6A}-KO), the AlexaFluor488 signal
174 corresponding to FLAG was weak and non-specific, i.e. appearing throughout the cell including in
175 the flagella (Supplementary Fig. 3a). In contrast, the c_{6A}-FLAG overexpressing sample (c_{6A}-OE)
176 showed a more intense (2 to 3-fold pixel intensity) and more localized fluorescence signal,
177 confirming chloroplast-specific localization of c_{6A} (Supplementary Fig. 3b). Two cells covering the
178 variation of AlexaFluor488 signal intensity were chosen as representatives to capture cell to cell
179 differences that could arise from technical variation from fixing and staining or c_{6A}-FLAG
180 expression level differences between cells. Nevertheless, the absence of AlexaFluor488 signal from
181 cell compartments other than the chloroplast in c_{6A}-OE compared to c_{6A}-KO supports the FLAG-
182 specificity of the signal. The detection of anti-FLAG signal in structures resembling pyrenoid-
183 traversing thylakoids supports a thylakoid luminal localization of the soluble
184 c_{6A} (Supplementary Fig. 3c-d). While it cannot be excluded that c_{6A} is associated with the thylakoid
185 membrane on the stromal side, the structure of c_{6A} (Fig. 1b) gives no indication of membrane-
186 association.
187 To detect possible covalent or strongly bound interaction partners, we performed co-
188 immunoprecipitation (co-IP) analyses of the c_{6A}-FLAG overexpressing strain (c_{6A}-OE) and the
189 untransformed background strain (c_{6A}-KO) using anti-FLAG-agarose beads. Immunodetection of
190 FLAG in the precipitate revealed bands at ~15 kDa in c_{6A}-OE but not in c_{6A}-KO, corresponding to
191 mature c_{6A}-FLAG (red arrows in Supplementary Fig. 4), with additional FLAG signals that were
192 not c_{6A}-FLAG specific in the 25-35 kDa range (black arrows in Supplementary Fig. 4). Under both

193 standard (Supplementary Fig. 4c) and DISCO Light (Supplementary Fig. 4f) conditions, the
194 immunoprecipitate did not reveal any bands unique to c_{6A}-OE except the c_{6A}-FLAG band,
195 indicating that no specific interaction partners of c_{6A} were detected.
196 The combined immunofluorescence microscopy and co-IP results indicate that c_{6A} is likely to be
197 localized in the thylakoid lumen, as for *A. thaliana* (23) and are consistent with any hypothesized
198 function relying primarily on weak or transient interactions.
199
200
201 <u>c_{6A} is important to maintain the light harvesting balance between photosystems I and II in</u>
202 <u>photomixotrophy</u>
203
204 Given the light-dependent growth phenotype observed in DISCO conditions, the likely localization
205 of c_{6A} in the thylakoid lumen, and c_{6A}'s high sequence similarity to c_6 which is involved in the
206 PETC, we investigated the photosystems and light harvesting complexes to explore further a
207 potential role of c_{6A} in photosynthesis.
208 We recorded low temperature (77K) chlorophyll fluorescence emission spectra. When grown in
209 continuous light (30 $\mu mol_{photons}$ m^{-2} s^{-1}) under photoautotrophic conditions WT and c_{6A}-KO
210 exhibited very similar fluorescence spectra (Fig. 2a, PSI/PSII fluorescence ratios 1.25 and 1.3,
211 respectively, P = 0.374), consistent with similar growth (Fig. 1c). However, when grown in
212 photomixotrophic conditions and continuous light (30 $\mu mol_{photons}$ m^{-2} s^{-1}, standard conditions), and
213 despite the two strains showing similar growth (Fig. 1b), WT maintained a PSI/PSII fluorescence
214 ratio of about 1.2, while c_{6A}-KO showed a significantly lower ratio (0.96, P = 0.008), which was
215 accompanied by a more prominent CP47-associated peak at 695 nm (33) (Fig. 2a). The PSI/PSII
216 fluorescence ratio was restored to nearly WT levels in the c_{6A}-OE strain (Fig. 2a). When samples
217 were grown in DISCO Light and photomixotrophy, the differences seen in standard conditions
218 were amplified. By day 4, the PSI/PSII fluorescence ratio in c_{6A}-KO dropped drastically to 0.66 in
219 comparison to WT and c_{6A}-OE (1.05 and 1.33, respectively & P = 0.027 and 0.0005, respectively).
220 Interestingly, WT showed a shoulder peak at ~681 nm (Fig. 2a), which may reflect partial
221 detachment of light harvesting complex II (LHCII) from PSII (34). The lower level of normalized
222 PSI fluorescence in c_{6A}-KO in all photomixotrophic samples did not originate from lower PSI
223 protein levels, as evidenced by PSI subunit immunoblot analyses (Supplementary Fig. 5).
224 To investigate if this c_{6A}-dependent light harvesting phenotype was due to alterations in state
225 transitions in photomixotrophy, for example due to c_{6A}-KO being locked in state 1, we induced

226 either state 1 (darkness and oxia) or state 2 (darkness and anoxia) in samples grown under standard
227 conditions (Fig. 2b). Both strains showed, as expected, a lower PSI/PSII fluorescence ratio in state
228 1 and a higher PSI/PSII fluorescence ratio in state 2, reflecting the increased sizes of the antenna
229 cross section of PSII and PSI, respectively. However, c_{6A}-KO consistently exhibited a lower
230 PSI/PSII fluorescence ratio than WT (Fig. 2c). Whereas WT exhibited PSI fluorescence of
231 1.13 (normalized to PSII fluorescence) in state 2 conditions, c_{6A}-KO showed a significantly lower
232 value of 1.01 ($P = 0.046$). Similarly, under state 1 inducing conditions, normalized PSI fluorescence
233 in WT was 0.85, compared to 0.77 in c_{6A}-KO ($P = 0.071$). While the CP47-associated peak at
234 695 nm (33) showed different intensity between the two states in WT, in c_{6A}-KO the same peak
235 intensity was recorded in both states.
236
237 As the light harvesting balance is affected by photosystem complex abundance and composition,
238 we next analyzed the thylakoid membrane complexes from cells grown in standard conditions using
239 BN-PAGE. Gels showed a distinct green band containing a PSI complex without LHCs (band III
240 marked red, Fig. 2d&e) that was consistently more prominent in c_{6A}-KO compared to WT and c_{6A}-
241 OE. The other bands showed a similar pattern and thus presumably similar photosystem complex
242 levels across strains (Fig. 2d). 2D-PAGE analyses and gel simulations to calculate the predicted
243 mobility in the gel (R_f) revealed similar subunit compositions of the complexes between
244 strains (Fig. 2e & Supplementary Fig. 7a-b).
245 Together, these results show that c_{6A} is important for maintaining the light harvesting balance
246 between the photosystems in photomixotrophic conditions, especially in combination with DISCO
247 light, and indicate that an altered distribution of LHCs could underly this observation.
248

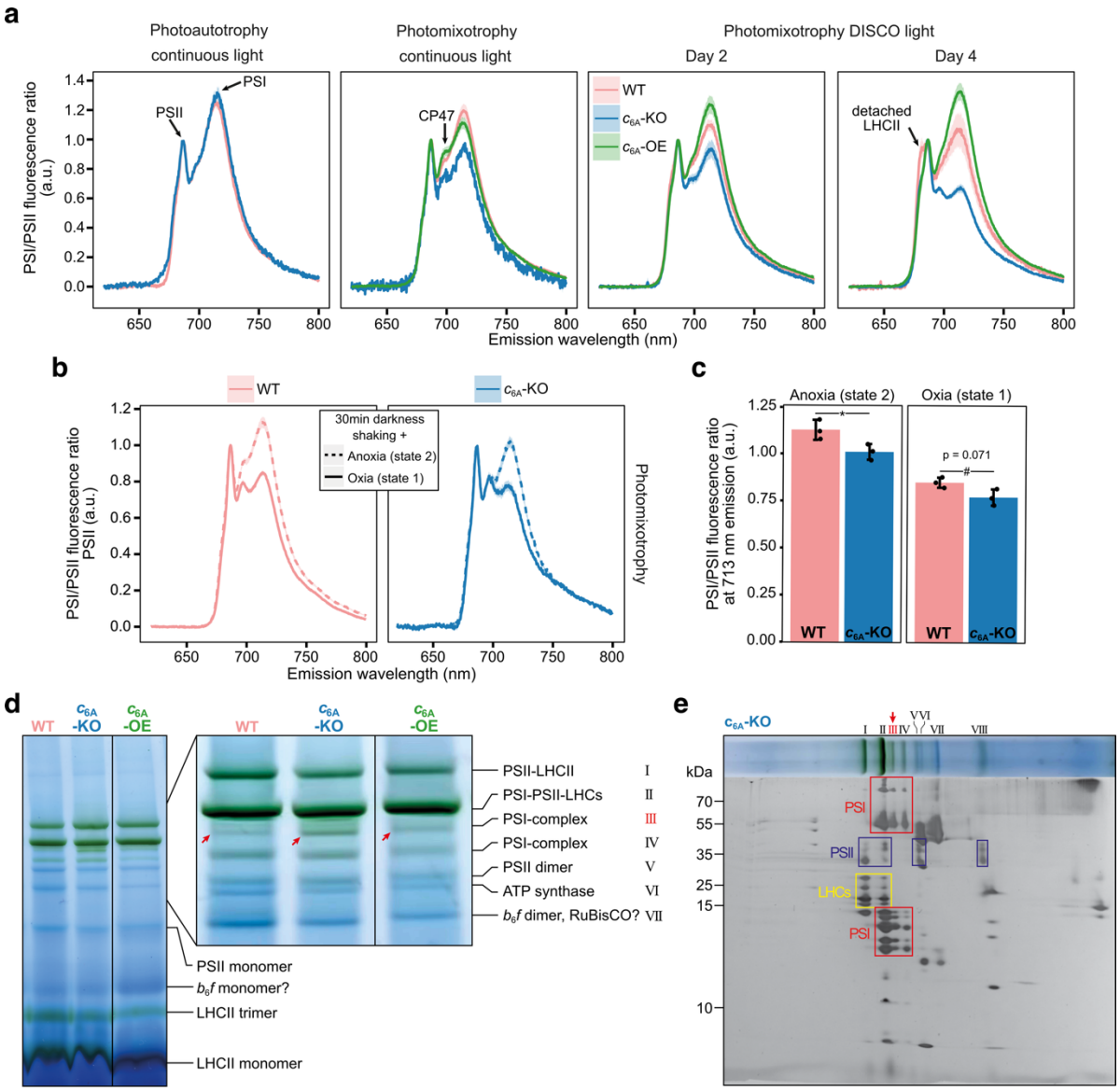

Figure 2: *c*6A affects the light harvesting balance between photosystems I and II in photomixotrophy. **a**, Low temperature (77 K) chlorophyll fluorescence spectra (excitation: 440 nm) of c_{6A} mutant strains and WT from cells grown under continuous light (30 $\mu mol_{photons}$ m^{-2} s^{-1}) in photoautotrophy -or mixotrophy and cells grown photomixotrophically under DISCO Light for 2 or 4 days. The prominent PSI and PSII fluorescence peaks of note are indicated by black arrows. **b**, Low temperature (77 K) chlorophyll fluorescence spectra of c_{6A}-KO and WT exposed to state 1 or 2 inducing conditions (n = 3 biological replicates ±SE). **c**, Quantification of the PSI to PSII fluorescence ratio at 713 nm from **b**. Statistical testing was carried out with a two-sided t-test per state ($p < 0.05$: *, $p < 0.1$: #). **d**, BN-PAGE analysis of c_{6A} mutant strains and WT thylakoid membrane complexes isolated from cells grown in photomixotrophy and continuous light (30 $\mu mol_{photons}$ m^{-2} s^{-1}). The inset shows the area of interest with band III from a separate longer BN-PAGE run with the same samples. The full gels with three biological replicates per strain can be found in Supplementary Figure 6. Thylakoid membrane complexes were assigned to bands according to the literature (53–55). **e,** 2D-PAGE analysis of a BN-PAGE lane from c_{6A} -KO with the boxes indicating assignment of spots to protein complexes based on comparison with calculated R_f values of known thylakoid membrane complex components (Supplementary Fig. 7c).

265 Absence of c_{6A} leads to a more reduced PQ pool

266

267 Given the tight link between light harvesting balance and the redox state of the PQ pool, we
268 quantified the redox state of the PQ pool using chlorophyll fluorescence measurements.
269 Firstly, the chlorophyll fluorescence induction (OJIP) traces of cells grown in standard conditions
270 revealed a 10% increase in the F_J parameter in c_{6A}-KO compared to WT and c_{6A}-OE ($P = 0.012$ and
271 0.008, respectively) (Fig. 3a,b). Since F_J reflects the extent of Q_A reduction and is positively
272 correlated with PQ pool reduction (35), this increase indicates that the absence of c_{6A} led to a more
273 reduced PQ pool.
274 To investigate further the extent of c_{6A}-dependent PQ pool overreduction, we exposed cells grown
275 in standard conditions to DISCO light and recorded chlorophyll fluorescence. The value of the
276 steady-state fluorescence yield F' under actinic light is influenced by the redox state of the PQ pool,
277 as the PQ pool is in a redox equilibrium with Q_A in PSII (36). During the high light periods of
278 DISCO Light, F' was on average 36% higher in c_{6A}-KO than in WT ($P = 0.0006$), indicating a more
279 reduced PQ pool in the absence of c_{6A} in DISCO Light as well (Fig. 3c). Also during the high light
280 periods of the DISCO Light regime, 1-qL (a measure of Q_A reduction) was high in WT (0.9)
281 indicating that Q_A and by implication the PQ pool was highly reduced (37). In c_{6A}-KO 1-qL was
282 significantly higher (0.975) again compared to WT ($P = 6.8 \times 10^{-5}$) (Fig. 3d), indicating a more
283 reduced PQ pool, consistent with the F' finding.
284 These results suggest that the absence of c_{6A} leads to a more reduced PQ pool in *Chlamydomonas*
285 under photomixotrophic conditions, exacerbated by DISCO Light exposure. Consequently, the
286 more reduced Q_A pool could lead to increased damage to PSII, potentially contributing to the
287 observed growth penalty in DISCO Light.

288

289

290 Redox kinetics of *b* hemes are affected and PSII quantum yield lowered in absence of c_{6A}

291

292 Given the effects of the absence of c_{6A} on light harvesting and PQ pool redox balance, we also
293 assessed the function of PETC complexes. We first measured the redox kinetics of cytochrome b_6f
294 using a Joliot-type spectrometer (JTS).
295 In photoautotrophic samples grown under continuous light (30 $\mu mol_{photons}$ m^{-2} s^{-1}), all strains
296 exhibited a *b* hemes reduction peak within 100 ms of light exposure, but in c_{6A}-KO the peak was
297 only half the intensity of WT (Supplementary Fig. 8). In samples grown in standard

photomixotrophic conditions, the *b* hemes in WT and c_{6A}-OE were reduced within 100 ms of light exposure followed by transient oxidation and re-reduction. In contrast, the *b* hemes in c_{6A}-KO were *oxidized* within 100 ms of illumination (Fig. 3e) and showed nearly no re-reduction in the following 500 ms. Interestingly, no differences in the cytochrome *f* redox kinetics were observed in either photoautotrophy or photomixotrophy (Supplementary Fig. 8), indicating no effect of the absence of c_{6A} on the function of the high potential chain.

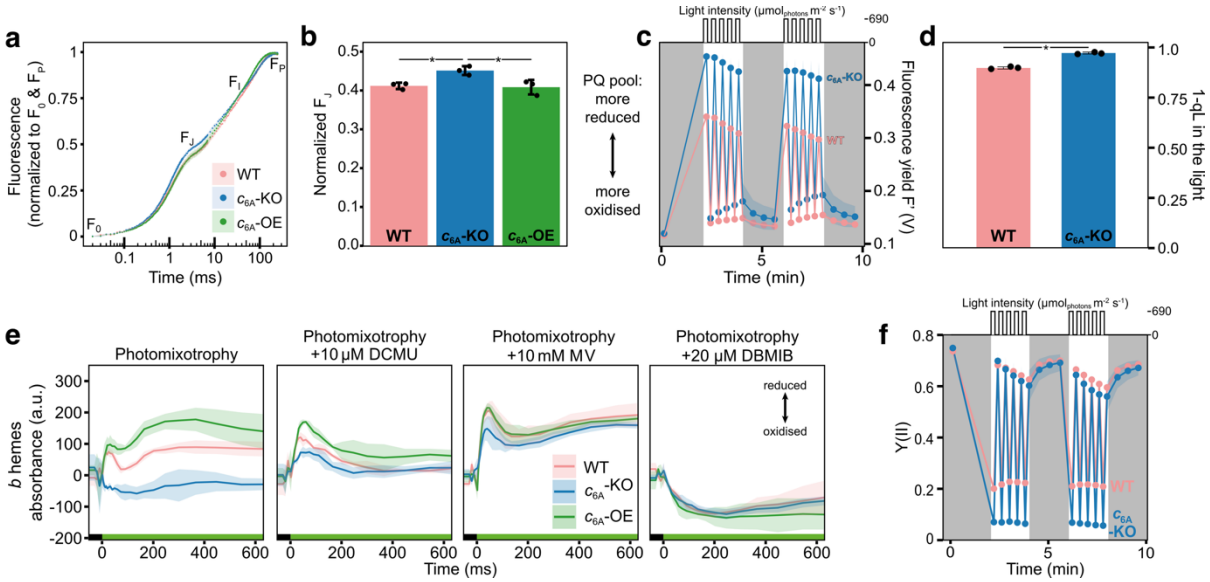

Figure 3: c_{6A} affects the redox state of the PQ pool, the redox kinetics of *b* hemes in cytochrome b_6f and the quantum yield of PSII. a, Chlorophyll fluorescence induction measurements (OJIP curves) of c_{6A} mutant strains and WT grown under photomixotrophic continuous light (30 $\mu mol_{photons}$ m^{-2} s^{-1}) conditions and normalized to F_0 and F_P (n = 3 biological replicates ±SD). **b**, Comparison of the normalized fluorescence at inflection point F_J (2.4 ms) from **a**. Asterisks indicate a significant difference ($p < 0.05$) as determined by one-way ANOVA and post-hoc pairwise two-sided t-test (n = 3 biological replicates ±SD). **c**, Raw steady-state fluorescence yield F' in Volts (V) of c_{6A}-KO and WT grown under standard conditions and exposed to a DISCO Light regime (on top of box) in a DUAL-PAM-100 spectrometer (n = 3 biological replicates ±SD). **d**, 1-qL values in the light phases of c_{6A}-KO and WT grown under standard conditions and exposed to the same light protocol as in **c** (n = 3 biological replicates ±SD, asterisk: significant difference ($p < 0.001$) as determined by two-sided t-test). **e**, Redox changes of *b* hemes in c_{6A} mutant strains and WT grown under standard conditions and exposed to DCMU (competitive inhibitor of the Q_B site in PSII), methyl viologen (MV, electron acceptor of PSI) or dibromothymoquinone (DBMIB, b_6f Q_P site blocker). Samples were exposed to green light (500 $\mu mol_{photons}$ m^{-2} s^{-1}, green bar) in a JTS-10 spectrometer (n = 3 biological replicates ±SD). **f**, Photosystem II quantum yield, Y(II), of c_{6A}-KO and WT grown under standard conditions and exposed to the same light protocol as in **c** (n = 3 biological replicates ±SD).

A more reduced PQ pool leads to lower reduction and even apparent oxidation of the *b* hemes upon light exposure (38–40). The latter is likely due to *b* hemes being pre-reduced in conditions with a highly reduced PQ pool. Thus, the effect of the absence of c_{6A} on the redox kinetics of *b* hemes are consistent with the observed change in the redox state of the PQ pool. Artificial modulation of the PQ pool redox state should therefore lead to smaller differences in *b* hemes redox kinetics between the strains. In the presence of dichlorophenyl-dimethylurea (DCMU), a PSII inhibitor that leads to

328 PQ pool oxidation, samples grown in standard conditions showed that the *b* hemes in c_{6A}-KO were
329 indeed reduced upon illumination but to a lower magnitude than in WT/ c_{6A}-OE (Fig. 3e). Similarly,
330 when we added methyl viologen (MV), an artificial electron acceptor from PSI that also leads to
331 PQ pool oxidation, the *b* hemes reduction was partially restored in in c_{6A}-KO (Fig. 3e).
332 Furthermore, when we added dibromothymoquinone (DBMIB), which blocks the Q_P site of
333 cytochrome b_6f and leads to PQ pool reduction, the *b* hemes only showed oxidation upon
334 illumination without differences between the strains (Fig. 3e).
335 The observed differences in *b* hemes redox kinetics can therefore be explained by the more reduced
336 PQ pool in c_{6A}-KO. Further, these results indicate that in the absence of c_{6A} the cytochrome b_6f
337 complex including the Q-cycle is in principle functional if the PQ pool is oxidized. Nevertheless,
338 small differences between c_{6A}-KO and WT/ c_{6A}-OE remained when the PQ pool was artificially
339 oxidized, warranting further investigation of the Q-cycle.
340
341 To investigate the possibility of a disturbed Q-cycle underlying the *b* hemes phenotype, we
342 measured the proton motive force (*pmf*) and its components of *Chlamydomonas* cells grown in
343 standard conditions using electrochromic shift (ECS) measurements. No substantial difference
344 between presence and absence of c_{6A} was detected in *pmf*, proton flux (vH^+) and thylakoid
345 conductivity (gH^+) when samples were exposed to either continuous red light (53 $\mu mol_{photons}$ m^{-2}
346 s^{-1}) or DISCO Light conditions (Supplementary Fig. 9a-f). Further, no differences between the
347 strains were found in the response of the ECS signal to a single turnover flash and the partitioning
348 of *pmf* into ΔpH and ΔΨ (Supplementary Fig. 9g&h). Together, this is consistent with c_{6A} not
349 affecting Q-cycle function.
350
351 We also analyzed the efficiency of photosystems I and II of *Chlamydomonas* cells grown in
352 standard conditions when exposed to continuous or DISCO Light. In continuous light, we did not
353 find any significant differences between WT and c_{6A}-KO in the quantum yield of PSII
354 (Supplementary Fig. 10a) and PSI (Supplementary Fig. 10b) over a wide range of intensities. There
355 was, however, an elevated photosystem II quantum yield Y(II) for c_{6A}-OE in comparison to c_{6A}-
356 KO at higher light intensities (above 210 $\mu mol_{photons}$ s^{-1} m^{-2}) resulting in an increased relative
357 electron transport rate (rETRII). Conversely, during the high light periods of DISCO Light, Y(II)
358 was less than half in c_{6A}-KO compared to WT (Fig. 3f). In contrast to PSII, PSI quantum yield Y(I)
359 was not majorly affected by absence of c_{6A} and DISCO Light and showed a decreasing trend in the
360 light phases from 0.2 to about 0.125 over the course of 40 min in both WT and c_{6A}-KO

361 (Supplementary Fig. 11). For both strains, DISCO Light led to an increase in acceptor side
362 limitation Y(NA), indicating that in DISCO Light downstream electron acceptors are not readily
363 available (Supplementary Fig. 11). Consistent with the more reduced PQ pool in absence of c_{6A},
364 c_{6A}-KO exhibited a lower donor-side limitation Y(ND) than WT during DISCO Light treatment
365 (Supplementary Fig. 11).
366 The DISCO Light condition therefore seems to lead to inhibition of photosynthesis at PSII in c_{6A}-
367 KO which is consistent with the highly reduced PQ pool in absence of c_{6A}.
368
369
370 <u>c_{6A} partly alleviates the stressful effect of DISCO Light on PSII</u>
371
372 To determine if the more reduced PQ pool in the absence of c_{6A} causes stress for *Chlamydomonas*
373 and could explain the observed growth phenotype, we measured PSII energy partitioning of cells
374 grown in standard conditions and then exposed to DISCO Light using a DUAL-PAM.
375 Increased stress levels in the absence of c_{6A} were evident when examining the quantum yield of
376 non-regulated dissipation of excitation energy, Y(NO), which describes the fraction of energy that
377 is neither used for photochemistry nor dissipated as heat in a regulated manner via NPQ. At the
378 start of DISCO Light exposure, over 90% of light energy was dissipated in a non-regulated fashion
379 in c_{6A}-KO, while WT had values below 80% (Fig. 4a). Over 40 minutes of DISCO Light, Y(NO)
380 levels in c_{6A}-KO relaxed, nearing WT levels of about 70%. High Y(NO) levels indicate PSII
381 photoinhibition that is imminent or has already occurred due to over-reduction (41). When probing
382 for PsbA, C-terminal fragments forming two bands at around 15 kDa were visible (Fig. 4b). An
383 increased ratio of PsbA (D1) degradation products to full length PsbA (D1) protein, which is
384 indicative of PSII photoinhibition (42), was observed in c_{6A}-KO on Day 4 of DISCO Light exposure
385 (Fig. 4b & Supplementary Fig. 12). In c_{6A}-KO, 20% of the observed PsbA (D1) protein signal
386 originated from the C-terminal fragment bands, while in WT and c_{6A}-OE the C-terminal fragments
387 only contributed 8% and 7% to the total PsbA (D1) signal, respectively (Supplementary Fig. 12).
388 The yield of regulated non-photochemical quenching Y(NPQ) was negligible in dark-adapted WT
389 and c_{6A}-KO samples (Fig. 4b). However, over the first 40 min of DISCO Light exposure, c_{6A}-KO
390 exhibited approximately twice the Y(NPQ) levels as WT during all phases of the DISCO Light
391 protocol. This sustained Y(NPQ) response, even in the dark, indicates increased stress levels in the
392 absence of c_{6A}, leading to an amplified engagement of NPQ mechanisms to allow energy dissipation
393 in a regulated manner. Interestingly, increased Y(NPQ) in the absence of c_{6A} was also observed

under a range of continuous light intensities, which was partially restored in the c_{6A}-OE strain (Supplementary Fig. 10a). Elevated NPQ levels in the absence of c_{6A} were further supported by an approximately 1.5-fold protein level of the NPQ effector LHCSR3 (43) in c_{6A}-KO compared to WT after two days of growth in DISCO Light (Fig. 4b & Supplementary Fig. 12).

Together, these data indicate that PSII experiences more photoinhibition in c_{6A}-KO than WT and c_{6A}-OE under DISCO Light consistent with the observed reduced Y(II) in c_{6A}-KO under DISCO Light (Fig. 3f). Increased photoinhibition is likely contributing to the observed growth penalty (Fig. 1c).

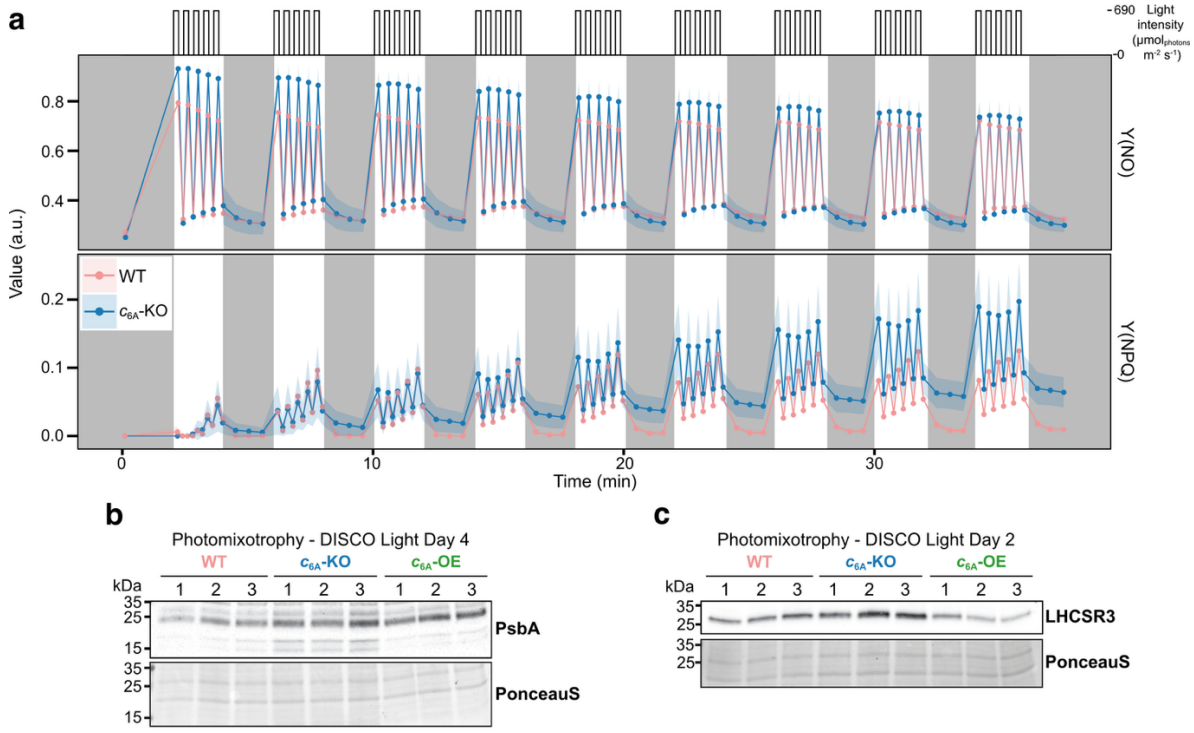

Figure 4: c_{6A} partly alleviates the stressful effect of DISCO Light on *Chlamydomonas*. a, Regulated non-photochemical quenching Y(NPQ), and non-regulated energy dissipation Y(NO) of c_{6A}-KO and WT grown under standard conditions and exposed to a DISCO Light regime in a DUAL-PAM-100 spectrometer (n = 3 biological replicates ±SD). **b**, Immunoblot analyses probing for PsbA in whole cell protein samples from c_{6A} mutant strains and WT grown in DISCO Light for four days (n = 3 biological replicates, PonceauS stain as total protein loading control). **c**, Immunoblot analyses probing for LHCSR3 in whole cell protein samples from c_{6A} mutant strains and WT grown in DISCO Light for two days (n = 3 biological replicates, PonceauS stain as total protein loading control). Relative quantification of the share of signal from C-terminal fragments for PsbA or the signal intensities normalized to total protein for LHCSR3 and can be found in Supplementary Figure 12.

416 **Discussion**

417

418 Here we present an in-depth characterization of the physiological role of the highly conserved
419 cytochrome c_{6A} protein in relation to photosynthesis and show that it is important for optimal
420 growth in fluctuating light due to its effect on the light harvesting and PQ pool redox state balances
421 of the model alga *Chlamydomonas* (summary see Supplementary Table 1).
422 Analysis of the redox state of the PQ pool using complementary chlorophyll fluorescence
423 approaches indicated that the PQ pool was more reduced in c_{6A}-KO, and this was particularly
424 marked in the high light periods of DISCO Light. JTS measurements of the redox state of the
425 *b* hemes of the cytochrome b_6f complex in response to light exposure showed disturbance of the
426 redox kinetics in the c_{6A}-KO that were consistent with a more reduced PQ pool in c_{6A}-KO. Addition
427 of DCMU or MV, which would be expected to lead to PQ oxidation, or DBMIB, which leads to
428 PQ reduction, revealed effects consistent with an increased pre-reduction of the *b* hemes in c_{6A}-KO
429 through a more reduced PQ pool. c_{6A}-KO exhibited no change in the proton motive force, measured
430 by electrochromic shift, rendering unlikely a direct effect of c_{6A} on the Q cycle. Under the high
431 light periods of DISCO Light, c_{6A}-KO showed a dramatic decrease in PSII quantum yield compared
432 to WT, which would also be consistent with a more reduced PQ pool. The c_{6A}-KO did not exhibit
433 any significant difference in PSI quantum yield under DISCO light, although it showed a decrease
434 in donor-side limitation of PSI, again consistent with a more reduced PQ pool. c_{6A}-KO also showed
435 some indication of increased acceptor-side limitation.
436 c_{6A}-KO exhibited an increase in the non-regulated dissipation of excitation energy [Y(NO)] and
437 regulated non-photochemical quenching [Y(NPQ)] with the onset of DISCO Light, as well as a
438 relative increase in the amount of the NPQ effector LHCSR3 protein and degradation products of
439 PsbA after two and four days of growth in DISCO Light, respectively. These results indicate an
440 increased tendency to photoinhibition in c_{6A}-KO, which might be accounted for by the increased
441 PQ reduction. A general impairment of PSII function or repair in the absence of any other effects
442 from loss of c_{6A} might be expected to lead to a decreased reduction in PQ. This suggests that the
443 PSII impairment is a consequence of the increased PQ reduction resulting from loss of c_{6A}, rather
444 than the primary result of c_{6A} loss.
445 What might cause the increase in reduction of the PQ pool in the absence of c_{6A}? The 77K
446 chlorophyll fluorescence data indicated a significantly lower PSI/PSII fluorescence ratio in c_{6A}-KO
447 compared to WT under photomixotrophic conditions, and this difference was amplified under
448 DISCO Light conditions. In BN-PAGE, a band corresponding to a LHC-less PSI was more

449 prominent in c_{6A}-KO than WT and c_{6A}-KO showed a lower PSI/PSII fluorescence value than the
450 wild type under both state 1 and state 2 conditions. These data are consistent with the photosystems
451 being preferentially in the equivalent of state 1 in c_{6A}-KO compared to WT. However, there was
452 no evidence for the c_{6A}-KO being permanently 'locked' in either state 1 or state 2.
453 Overall, it therefore seems likely that c_{6A}-KO is disturbed in the light harvesting balance between
454 PSI and PSII, in favor of PSII, especially under DISCO Light. This leads to a more reduced PQ
455 pool, and consequent photoinhibition, with impaired growth of c_{6A}-KO in DISCO conditions. c_{6A}
456 is likely to be located in the thylakoid lumen and has been shown to interact with the lumen thiol
457 oxidase LTO1 (21), which is closely involved in thiol-based regulation of the STT7 (STN7 in
458 Arabidopsis) state transition kinase, keeping STT7 oxidized (22). STT7 is active only when
459 oxidized and, in response to a reduced PQ pool, catalyzes phosphorylation of LHCII and causing
460 LHCII to move from PSII to PSI. c_{6A} has been proposed to catalyze the formation of disulfide
461 bridges in the lumen (10, 11), transferring electrons to plastocyanin, with which it has been shown
462 to react (19). Although we cannot exclude a more complex explanation, with the shift in PSI/PSII
463 balance and change in state of the PQ pool being indirect consequences of loss of c_{6A}, we propose
464 that c_{6A} contributes to oxidation of STT7. c_{6A} is not essential for the oxidation as state transitions
465 remain in c_{6A}-KO. However, it may be that c_{6A} assists in the transfer of electrons from STT7 to
466 LTO1 (with which it interacts (21)) or another acceptor. Thus, in the absence of c_{6A}, STT7 would
467 be more reduced than in WT, leading to increased light harvesting at PSII and a more reduced PQ
468 pool compared to WT. This model could be tested in the future by making substitutions to the
469 conserved cysteine residues in c_{6A}. If correct, this will be a significant contribution to our
470 understanding of the complex thiol-based regulatory network of the thylakoid lumen of
471 photosynthetic organisms (44). Furthermore, the demonstration of the importance of c_{6A} for growth
472 under fluctuating light conditions presents a significant contribution to understand how organisms
473 cope with rapidly changing light conditions (45, 46). The connection of c_{6A} to state transitions also
474 make it a significant target for optimizing crop productivity.
475
476
477 **Materials and Methods**
478
479 Growth conditions
480 *Chlamydomonas* strains were maintained on Tris-Acetate-Phosphate (TAP) (47) medium with
481 Hutner's trace element solution (48) supplemented with 1.5% agar at 30 $\mu mol_{photons}\ m^{-2}\ s^{-1}$ and

482 25 °C. For longer-term storage cultures were kept on TAP slants in ambient light at room
483 temperature. Liquid cultures were grown at 30 $\mu mol_{photons}\ m^{-2}\ s^{-1}$, 25 °C and 120 rpm in AlgaeTron
484 AG130 or AG230 incubators (Photon System Instruments) unless otherwise specified.
485 For experimental cultures, triplicates of 30 mL medium (Tris-phosphate (TP) medium (47) for
486 photoautotrophic, and TAP for photomixotrophic conditions) were inoculated with
487 *Chlamydomonas* strains to OD_{750nm} = 0.1. The cultures were then subjected to the experimental
488 conditions (Table 1). All experimental cultures were subcultured at least twice in standard
489 conditions before exposure to experimental conditions.
490 Table 1: Experimental light conditions in the AlgaeTron AG130 and AG230 growth chambers.

Name	**Light regime**
Standard growth light	continuous 30 $\mu mol_{photons}\ m^{-2}\ s^{-1}$
High light	continuous 700 $\mu mol_{photons}\ m^{-2}\ s^{-1}$
Darkness	continuous 0 $\mu mol_{photons}\ m^{-2}\ s^{-1}$
2 min on/off	alternating 2 min 700 $\mu mol_{photons}\ m^{-2}\ s^{-1}$ & 2 min darkness
12 s on/off	alternating 12 s 700 $\mu mol_{photons}\ m^{-2}\ s^{-1}$ & 12 s darkness
DISCO Light	alternating 2 min darkness & 2 min of 12 s 700 $\mu mol_{photons}\ m^{-2}\ s^{-1}$/ 12 s off (Fig. 1d)

491
492
493 Algal strains
494 The cytochrome c_{6A} knock-out strain "c_{6A}-KO" (CC-1883 background) was generated as previously
495 described (32) using the gRNAs 5'-ATTTACAGTTAGTGCATCCACTTG-3' and
496 5'-TCCGAGGGTAAGCAAGCACGGCAC-3' to target the 5'UTR and Exon III for Cpf1-
497 mediated double strand breaks, respectively. A repair template with the following sequence was
498 provided at the same time to introduce a multiple stop codon (lowercase letters):
499 5'-TCATGCTCGGCCAGTTTTCTTTGATTTCAAATCCTCGCTAATTTActaattaactaaCAGCT
500 TCCTTGCTTCATGGACCCAGTAACGGTGCATGGGTACGCG-3'.
501 The c_{6A}-overexpression strain c_{6A}-OE was created by transforming c_{6A}-KO with the constructs
502 pDKM-000 by electroporation as described before (49) and specified in the Supplementary
503 Methods.
504
505 Protein extraction and Western Blot
506 A known volume of *Chlamydomonas* cells at a desired growth stage was harvested by
507 centrifugation at 1000 xg for 5 min. The pellet was subsequently resuspended in RIPA lysis buffer

508 with freshly added PMSF (1mM final concentration) to reach a calculated OD_{750nm} of 50. The
509 chlorophyll content was measured as above, but here 10 µL of sample were mixed with 40 µL of
510 acetone and 1 mL of 80% acetone, resulting in a dilution factor D of 105. Protein samples were
511 then adjusted to the same total chlorophyll concentration with RIPA buffer and frozen at -20 °C for
512 at least 1.5 h or overnight, followed by thawing on ice to complete cell lysis. Protein concentration
513 was determined using a Bradford assay (Merck) according to manufacturer's instructions diluting
514 the protein samples 5- to 10-fold.
515 For SDS-PAGE, all samples were diluted to 1 µg/µL protein with RIPA buffer before being mixed
516 with 4x Lämmli buffer and incubated for 30 min (50 °C, 600 rpm). After centrifuging the samples
517 (12000 xg, 1 min) to remove insoluble material, samples were loaded to the desired amount into
518 wells of polyacrylamide gels (Mini-PROTEAN TGX Stain-Free, BioRad). PageRuler Plus (7 µL,
519 Thermo Scientific) was used as size marker. Electrophoresis was carried out at 4 °C and 200 V for
520 about 50 min. The gel was imaged in a ChemiDoc MP imaging system (BioRad) using the Stain
521 Free setting and 5 min activation time. Some gels were stained with Pierce™ Silver Stain for Mass
522 Spectrometry (Thermo Scientific).
523 Transfer of protein from polyacrylamide gels onto polyvinylidene fluoride (PVDF) membranes was
524 carried out using the iBlot dry transfer apparatus, following the manufacturer's instructions and
525 using program P3 for 5 min. Membranes were then probed for successful transfer with PonceauS
526 (Thermo Scientific) as per manufacturer's instructions and imaged with the ChemiDoc MP imaging
527 system (BioRad). Following the PonceauS destaining, membranes were blocked in 5% milk in Tris-
528 buffered saline with 0.1% Tween 20 (TBS-T) for 1 h at room temperature with gentle shaking.
529 After washing membranes once with TBS-T to remove remnants of blocking agent, membranes
530 were incubated with specific primary antibody solutions in 5% milk TBS-T overnight at 4 °C (PsaB
531 (AS10695, Agrisera) at 1:1000, PsbA D1 (AS05084, Agrisera) at 1:10000, LHCSR3 (AS142766,
532 Agrisera) at 1:2000). Subsequently, membranes were washed with TBS-T (5x 5 min) and incubated
533 for 1.5 h at room temperature with goat anti-rabbit horseradish peroxidase-linked secondary
534 antibody in 5% milk TBS-T (1:10000, 1706515, BioRad). After washing membranes thrice in TBS-
535 T and once in TBS (10 min each), they were incubated with chemiluminescence substrate
536 (SuperSignal™ West Pico PLUS Chemiluminescent Substrate, Thermo Scientific) and imaged
537 using a ChemiDoc MP imaging system (BioRad).
538
539 <u>Low temperature chlorophyll (77K) fluorescence</u>

540 77K fluorescence emission spectra were recorded with a QE Pro spectrophotometer (Ocean Optics,
541 Dunedin, FL, USA). Cell samples (200 µL) frozen in liquid N_2 were excited with blue light (440
542 nm). Raw spectra were normalized to the photosystem II (PSII) fluorescence peak at 685 nm.
543 *Chlamydomonas* cells were harvested and total chlorophyll concentration was adjusted to 5 µg/mL
544 with fresh medium (TP or TAP). Cells were then frozen in liquid N_2 for measurement.
545 For the state transition experiment, *Chlamydomonas* cells grown in TAP under standard conditions
546 were adjusted to 5 µg/mL total chlorophyll with fresh medium. Anoxia (state 2 inducing) samples
547 were adjusted with medium containing glucose (final concentration 20 mM) and Glucose Oxidase
548 (final concentration 50 U/mL) that was purged with N2 for 3 min. The final samples were again
549 purged with N_2 before being sealed. Oxia (state 1 inducing) samples were adjusted with unchanged
550 medium and left unsealed. All samples were then shaken for 30 min in darkness before being frozen
551 in liquid N_2 for fluorescence measurement.
552
553 Blue native PAGE and second dimension SDS-PAGE
554 Thylakoid membranes from *Chlamydomonas* cultures were isolated over a discontinuous Percoll
555 gradient as described before (50). BN-PAGE was then carried out largely as previously (51).
556 Thylakoid samples were diluted with resuspension buffer (25 mM Bis-Tris/HCl (pH 7.0), 20%
557 (w/v) glycerol, 0.25 mg/ml Pefabloc, and 10 mM sodium fluoride) to a chlorophyll concentration
558 of 0.53 µg/µL and to a total of 6 µg chlorophyll. An equal volume of β -dodecyl maltoside (β -DM,
559 2% in resuspension buffer) was added to each sample and the thylakoid membranes were
560 solubilized by gentle pipetting for 2 min. After centrifugation (4 °C, 18000 xg, 20 min) samples
561 were mixed with a one-tenth volume of sample loading buffer (100 mM Bis-Tris/HCl (pH 7.0), 0.5
562 M ACA, 30% (w/v) sucrose and 50 mg/ml Serva Blue G) and loaded into the wells of a
563 NativePAGE 3-12% Bis-Tris protein gel (Invitrogen). Electrophoresis was carried out with specific
564 anode buffer (50 mM Bis-Tris/HCl, pH 7.0) and cathode buffer containing Serva Blue G dye (50
565 mM Tricine, 15 mM Bis-Tris/HCl, pH 7.0, and 0.01% Serva Blue G) at 4 °C for 20 min at 75 V,
566 30 min at 100 V, 30 min at 125 V, 60 min at 150 V, 30 min at 175 V and 60 min at 200 V. After
567 the 30 min at 125 V, the blue cathode buffer was replaced by the same cathode buffer but without
568 Serva Blue G. The last step was prolonged to 5 h if additional separation of bands of interest was
569 needed.
570 Gel electrophoretic separation of complexes in BN-PAGE lanes on a second dimension SDS-PAGE
571 was carried out as previously described (51, 52), although 12% polyacrylamide gels were used
572 here. Gels were stained with Pierce™ Silver Stain (Thermo Scientific).

573 The predicted mobility in the gel (R_f) values of known thylakoid membrane complex components
574 were calculated using their known molecular weight and a linear regression of the distance of the
575 protein standard in relation to the running front ($r^2 = 0.98$). The 2D-PAGE spots were compared
576 with the R_f values and with published BN-PAGE analyses from *Chlamydomonas* (53–55) to assign
577 the bands and proteins.
578
579 Chlorophyll fluorescence
580 Chlorophyll fluorescence induction (OJIP) of *Chlamydomonas* was measured with a FL3500
581 fluorometer (Photon System Instruments). Prior to measurement, cells were resuspended in TAP
582 and total chlorophyll concentration was adjusted to 20 µg/mL. After recovery under standard
583 growth conditions for at least 30 min, chlorophyll concentration was readjusted to 5 µg/mL. After
584 15 min incubation in darkness, fluorescence induction in response to red light (984 $\mu mol_{photons}$ m^{-2}
585 s^{-1}, 45% A-voltage) was recorded for 120 s. Raw fluorescence data was double normalized to
586 fluorescence at time point 0 and the maximum fluorescence value to compare the kinetics between
587 samples (37).
588 Chlorophyll fluorescence of *Chlamydomonas* was measured with a pulse amplitude-modulated
589 spectrometer (Dual-PAM-100, Walz). Prior to measurements, cells were resuspended in TAP and
590 the chlorophyll concentration was adjusted to 20 µg/mL. After recovery under standard growth
591 conditions for at least 30 min, measurements were performed in a quartz cuvette at 25 °C with
592 stirring and samples were initially incubated in darkness for 5 min before the blue fluorescence
593 measuring light (Intensity 12, 28 $\mu mol_{photons}$ m^{-2} s^{-1}) was turned on. Saturating pulses (Intensity 5,
594 5000 $\mu mol_{photons}$ m^{-2} s^{-1}, 500 ms width) for PSII parameter determination were applied with stirring
595 turned off. DISCO Light conditions in the DUAL-PAM-100 were achieved by alternating 2 min
596 darkness followed by 2 min consisting of 12 s high light (690 $\mu mol_{photons}$ m^{-2} s^{-1}) and 12 s darkness
597 alternations. Saturating pulses were applied in the middle of each 12 s phase or three times during
598 the 2 min dark phases. F' was recorded as the fluorescence yield during illumination with the actinic
599 light treatment before application of a saturating pulse. Photosynthetic parameters were calculated
600 as described previously (41).
601
602 Cytochrome b_6f redox kinetics
603 Cytochrome *f* and *b* heme redox kinetics were determined in *Chlamydomonas* cells by
604 deconvoluting absorbance changes at 546, 554, 563, and 573 nm that were measured using a JTS-
605 10 pump probe spectrophotometer (BioLogic) and appropriate 10 nm FWHM (full width at half

606 maximum) interference filters (Edmund Optics). BG39 filters (Schott) were used to shield the light
607 detectors from scattered light. Prior to measurements, cells were resuspended in fresh medium to a
608 total chlorophyll concentration of 20 µg/mL. After recovery under standard growth conditions for
609 at least 30 min, Ficoll 400 was added to a final concentration of 10%. For some samples, DCMU,
610 methyl viologen, or DBMIB were added to a final concentration of 10 µM, 10 mM, or 20 µM
611 respectively, at the same time as Ficoll. Cells were dark-adapted for 3 min before measurement
612 with each interference filter and then illuminated with 5 s of green light (500 $\mu mol_{photons}\ m^{-2}\ s^{-1}$).
613 Flashes of white detection light were administered during 300 µs dark intervals in actinic
614 illumination. Every recording was corrected for any detection light impact by subtracting a trace
615 with actinic light turned off. Deconvolution was performed with the JTS-10 software by drawing a
616 baseline between 573 and 546 nm. During analysis, the signal-to-noise ratio was improved with a
617 Savitzky-Golay filter (56).
618
619
620 **Acknowledgments**
621
622 We thank Dr. K. Geissler (University of Cambridge) for the provision of the pCM0 MoClo parts
623 and Dr. J. Walter (University of Cambridge) for assistance with blue native PAGE. We are also
624 grateful to Dr. M. Jokel (University of Turku) for discussions on cell culture. All photosynthesis
625 experiments were performed within the PHOTOSYN infrastructure at the University of Turku. We
626 gratefully acknowledge the support of this work by: the Gates Cambridge Trust with support from
627 the Benn W Levy Trust, and the Professor John Glover Memorial Fund (to DK); the Novo Nordisk
628 Foundation (PhotoCat, project no. NNF20OC0064371, to YA; and Photo-e-microbes project no.
629 NNF22OCOO79717 to LTW); the Research Council of Finland no. 355335 to YA, no. 354876 to
630 LN; the Biotechnology and Biological Sciences Research Council (BB/M011194/1 to AS,
631 BB/M011194/1 to JML, BB/R506163/1 to AF, and BB/Y001370/1 to CJH), and Trinity Hall,
632 Cambridge (to JML).
633
634 **Author Contributions:** DK conceived the project, designed and performed experiments under
635 the supervision of CJH and YA, and analyzed data. DK, LTW, LN, and YA developed the
636 biophysical part of the project. LTW and LN supervised the biophysical measurements and
637 assisted with data analysis and interpretation. AF created the knock-out mutant line under the
638 supervision of AM. JML and AS assisted with data collection, analysis and interpretation. AM,

YA, and CJH secured funding, assisted with data interpretation, and provided resources. DK wrote the manuscript with comments and input from all authors.

Competing Interest Statement: The authors declare no competing interests.

References

1. M. Weigel, *et al.*, Plastocyanin is indispensable for photosynthetic electron flow in Arabidopsis thaliana. *J. Biol. Chem.* **278**, 31286–31289 (2003).

2. G. A. Peschek, C. Obinger, M. Paumann, The respiratory chain of blue-green algae (cyanobacteria). *Physiol. Plant.* **120**, 358–369 (2004).

3. R. Gupta, Z. He, S. Luan, Functional relationship of cytochrome c6 and plastocyanin in Arabidopsis. *Nature* **417**, 567–571 (2002).

4. J. Wastl, D. S. Bendall, C. J. Howe, Higher plants contain a modified cytochrome c6. *Trends Plant Sci.* **7**, 244–245 (2002).

5. J. Wastl, S. Purton, D. S. Bendall, C. J. Howe, Two forms of cytochrome c6 in a single eukaryote. *Trends Plant Sci.* **9**, 474–476 (2004).

6. I. Nimmo, Location and function of cytochrome c6A. *PhD Thesis Univ. Camb.* (2011).

7. C. J. Howe, R. H. Nimmo, A. C. Barbrook, D. S. Bendall, "Cytochrome c6A of Chloroplasts" in *Cytochrome Complexes: Evolution Structures, Energy Transduction and Signaling*, Advances in Photosynthesis and Respiration., W. A. Cramer, T. Kallas, Eds. (Springer Science+Business Media, 2016).

8. U. Hani, *et al.*, A complex and dynamic redox network regulates oxygen reduction at photosystem I in Arabidopsis. *Plant Physiol.* (2024). https://doi.org/10.1093/plphys/kiae501.

9. B. A. Slater, The ancestry and function of cytochrome c6A. *PhD Thesis Univ. Camb.* (2020).

10. C. J. Howe, B. G. Schlarb-Ridley, J. Wastl, S. Purton, D. S. Bendall, The novel cytochrome c6 of chloroplasts: a case of evolutionary bricolage? *J. Exp. Bot.* **57**, 13–22 (2006).

11. B. G. Schlarb-Ridley, R. H. Nimmo, S. Purton, C. J. Howe, D. S. Bendall, Cytochrome c 6A is a funnel for thiol oxidation in the thylakoid lumen. *FEBS Lett.* **580**, 2166–2169 (2006).

12. H. Chida, *et al.*, Crystal structure of oxidized cytochrome c 6A from Arabidopsis thaliana. *FEBS Lett.* **580**, 3763–3768 (2006).

13. J. A. R. Worrall, B. F. Luisi, B. G. Schlarb-Ridley, D. S. Bendall, C. J. Howe, Cytochrome c 6A: discovery, structure and properties responsible for its low haem redox potential. *Biochem. Soc. Trans.* **36**, 1175–1179 (2008).

672 14. J. M. Mason, D. S. Bendall, C. J. Howe, J. A. R. Worrall, The role of a disulfide bridge in the
673 stability and folding kinetics of Arabidopsis thaliana cytochrome c6A. *Biochim. Biophys. Acta*
674 *BBA - Proteins Proteomics* **1824**, 311–318 (2012).

675 15. J. A. R. Worrall, *et al.*, Modulation of Heme Redox Potential in the Cytochrome c 6 Family. *J.*
676 *Am. Chem. Soc.* **129**, 9468–9475 (2007).

677 16. B. Slater, D. Kosmützky, R. E. R. Nisbet, C. J. Howe, The Evolution of the Cytochrome c6
678 Family of Photosynthetic Electron Transfer Proteins. *Genome Biol. Evol.* **13**, 1–12 (2021).

679 17. F. P. Molina-Heredia, *et al.*, A new function for an old cytochrome? *Nature* **424**, 33–34 (2003).

680 18. J. Wastl, *et al.*, Redox properties of Arabidopsis cytochrome c6 are independent of the loop
681 extension specific to higher plants. *Biochim. Biophys. Acta BBA - Bioenerg.* **1657**, 115–120
682 (2004).

683 19. M. J. Marcaida, *et al.*, Structure of Cytochrome c6A, a Novel Dithio-cytochrome of Arabidopsis
684 thaliana, and its Reactivity with Plastocyanin: Implications for Function. *J. Mol. Biol.* **360**, 968–
685 977 (2006).

686 20. P. Pesaresi, *et al.*, Mutants, overexpressors, and interactors of arabidopsis plastocyanin isoforms:
687 Revised roles of plastocyanin in photosynthetic electron flow and thylakoid redox state. *Mol.*
688 *Plant* **2**, 236–248 (2009).

689 21. Y. Lu, *et al.*, Identification of Potential Targets for Thylakoid Oxidoreductase AtVKOR/LTO1 in
690 Chloroplasts. *Protein Pept. Lett.* **22**, 219–225 (2015).

691 22. J. Wu, *et al.*, Functional redox links between lumen thiol oxidoreductase1 and serine/threonine-
692 protein kinase STN7. *Plant Physiol.* **186**, 964–976 (2021).

693 23. P. J. Gollan, A. Trotta, A. A. Bajwa, I. Mancini, E.-M. Aro, Characterization of the Free and
694 Membrane-Associated Fractions of the Thylakoid Lumen Proteome in Arabidopsis thaliana. *Int.*
695 *J. Mol. Sci.* **22**, 8126 (2021).

696 24. J. Beltrán, *et al.*, Specialized Plastids Trigger Tissue-Specific Signaling for Systemic Stress
697 Response in Plants. *Plant Physiol.* **178**, 672–683 (2018).

698 25. M. Janssen, *et al.*, Efficiency of light utilization of Chlamydomonas reinhardtii under medium-
699 duration light/dark cycles. *J. Biotechnol.* **78**, 123–137 (2000).

700 26. P. J. Graham, B. Nguyen, T. Burdyny, D. Sinton, A penalty on photosynthetic growth in
701 fluctuating light. *Sci. Rep.* **7**, 1–11 (2017).

702 27. L. Nikkanen, *et al.*, PGR5 is needed for redox-dependent regulation of ATP synthase both in
703 chloroplasts and in cyanobacteria. [Preprint] (2025). Available at:
704 https://www.biorxiv.org/content/10.1101/2024.11.03.621747v2 [Accessed 29 March 2026].

705 28. M. Jokel, X. Johnson, G. Peltier, E. Aro, Y. Allahverdiyeva, Hunting the main player enabling
706 Chlamydomonas reinhardtii growth under fluctuating light. *Plant J.* **94**, 822–835 (2018).

29. C. J. Steen, A. Burlacot, A. H. Short, K. K. Niyogi, G. R. Fleming, Interplay between LHCSR proteins and state transitions governs the NPQ response in Chlamydomonas during light fluctuations. *Plant Cell Environ.* **45**, 2428–2445 (2022).

30. T. Roach, LHCSR3-Type NPQ Prevents Photoinhibition and Slowed Growth under Fluctuating Light in Chlamydomonas reinhardtii. *Plants* **9**, 1604 (2020).

31. W. J. Nawrocki, *et al.*, Chlororespiration Controls Growth Under Intermittent Light. *Plant Physiol.* **179**, 630–639 (2019).

32. A. Ferenczi, D. E. Pyott, A. Xipnitou, A. Molnar, Efficient targeted DNA editing and replacement in Chlamydomonas reinhardtii using Cpf1 ribonucleoproteins and single-stranded DNA. *Proc. Natl. Acad. Sci.* **114**, 13567–13572 (2017).

33. E. G. Andrizhiyevskaya, *et al.*, Origin of the F685 and F695 fluorescence in Photosystem II. *Photosynth. Res.* **84**, 173–180 (2005).

34. J. Kargul, J. Nield, J. Barber, Three-dimensional reconstruction of a light-harvesting complex I-photosystem I (LHCI-PSI) supercomplex from the green alga Chlamydomonas reinhardtii: Insights into light harvesting for PSI. *J. Biol. Chem.* **278**, 16135–16141 (2003).

35. S. Z. Tóth, G. Schansker, R. J. Strasser, A non-invasive assay of the plastoquinone pool redox state based on the OJIP-transient. *Photosynth. Res.* **93**, 193 (2007).

36. B. A. Diner, Dependence of the deactivation reactions of Photosystem II on the redox state of plastoquinone pool a varied under anaerobic conditions. Equilibria on the acceptor side of Photosystem II. *Biochim. Biophys. Acta BBA - Bioenerg.* **460**, 247–258 (1977).

37. H. M. Kalaji, *et al.*, Frequently asked questions about chlorophyll fluorescence, the sequel. *Photosynth. Res.* **132**, 13–66 (2017).

38. P. Joliot, A. Joliot, Proton pumping and electron transfer in the cytochrome bf complex of algae. *Biochim. Biophys. Acta BBA - Bioenerg.* **849**, 211–222 (1986).

39. F. Buchert, M. Scholz, M. Hippler, Electron transfer via cytochrome b 6 f complex displays sensitivity to antimycin A upon STT7 kinase activation. *Biochem. J.* **479**, 111–127 (2022).

40. A. Malnoë, F.-A. Wollman, C. de Vitry, F. Rappaport, Photosynthetic growth despite a broken Q-cycle. *Nat. Commun.* **2**, 301 (2011).

41. C. Klughammer, U. Schreiber, Complementary PS II quantum yields calculated from simple fluorescence parameters measured by PAM fluorometry and the Saturation Pulse method. *PAM Appl. Notes* **1**, 27–35 (2008).

42. W. J. Nawrocki, *et al.*, Molecular origins of induction and loss of photoinhibition-related energy dissipation q I. *Sci. Adv.* **7**, 1–13 (2021).

43. M. Ballottari, *et al.*, Identification of pH-sensing Sites in the Light Harvesting Complex Stress-related 3 Protein Essential for Triggering Non-photochemical Quenching in Chlamydomonas reinhardtii. *J. Biol. Chem.* **291**, 7334–7346 (2016).

44. D. Hoh, J. E. Froehlich, D. M. Kramer, Redox regulation in chloroplast thylakoid lumen: The pmf changes everything, again. *Plant Cell Environ.* **47**, 2749–2765 (2024).

45. N. A. Eckardt, *et al.*, Lighting the way: Compelling open questions in photosynthesis research. *Plant Cell* **14**, 1–16 (2024).

46. S. P. Long, *et al.*, Into the Shadows and Back into Sunlight: Photosynthesis in Fluctuating Light. *Annu. Rev. Plant Biol.* **73**, 617–648 (2022).

47. D. S. Gorman, R. P. Levine, Cytochrome f and plastocyanin: their sequence in the photosynthetic electron transport chain of Chlamydomonas reinhardi. *Proc. Natl. Acad. Sci.* **54**, 1665–1669 (1965).

48. S. H. Hutner, L. Provasoli, A. Schnatz, C. P. Haskins, Some Approaches to the Study of the Role of Metals in the Metabolism of Microorganisms. *Proc. Am. Philos. Soc.* **94**, 152–170 (1950).

49. P. Crozet, *et al.*, Birth of a Photosynthetic Chassis: A MoClo Toolkit Enabling Synthetic Biology in the Microalga *Chlamydomonas reinhardtii*. *ACS Synth. Biol.* **7**, 2074–2086 (2018).

50. C. B. Mason, T. M. Bricker, J. V. Moroney, A rapid method for chloroplast isolation from the green alga Chlamydomonas reinhardtii. *Nat. Protoc.* **1**, 2227–2230 (2006).

51. S. Järvi, M. Suorsa, V. Paakkarinen, E. M. Aro, Optimized native gel systems for separation of thylakoid protein complexes: Novel super- and mega-complexes. *Biochem. J.* **439**, 207–214 (2011).

52. M. Rantala, V. Paakkarinen, E. M. Aro, Analysis of thylakoid membrane protein complexes by blue native gel electrophoresis. *J. Vis. Exp.* **2018**, 1–6 (2018).

53. E. Devadasu, *et al.*, Long- and short-term acclimation of the photosynthetic apparatus to salinity in Chlamydomonas reinhardtii. The role of Stt7 protein kinase. *Front. Plant Sci.* **14**, 1–17 (2023).

54. J. G. García-Cerdán, *et al.*, A thylakoid membrane-bound and redox-active rubredoxin (RBD1) functions in de novo assembly and repair of photosystem II. *Proc. Natl. Acad. Sci. U. S. A.* **116**, 16631–16640 (2019).

55. B. Spaniol, *et al.*, Complexome profiling on the Chlamydomonas lpa2 mutant reveals insights into PSII biogenesis and new PSII associated proteins. *J. Exp. Bot.* **73**, 245–262 (2022).

56. M. J. E. Savitzky, A.; Golay, Smoothing and Differentiation of Data. *Anal Chem* **36**, 1627–1639 (1964).

57. C. A. Kerfeld, H. P. Anwar, R. Interrante, S. Merchant, T. O. Yeates, The Structure of Chloroplast Cytochrome c6 at 1.9 Å Resolution: Evidence for Functional Oligomerization. *J. Mol. Biol.* **250**, 627–647 (1995).